Structural Engineering and Mechanics, Vol. 6, No. 4 (1998) 363-375
DOI: http://dx.doi.org/10.12989/sem.1998.6.4.363

Contact surface element method for two-dimensional elastic contact problems

Zhengxing Liu† and Yaowen Yang‡†

Department of Engineering Mechanics, Shanghai Jiao Tong University, Shanghai 200030, China

F.W. Williams‡ and A.K. Jemah‡‡

Division of Structural Engineering, Cardiff School of Engineering, University of Wales Cardiff, Cardiff CF2 3TB, U.K.

Abstract. The stiffness matrix of a two-dimensional contact surface element is deduced from the principle of virtual work. The incremental loading procedure used is controlled by displacement and stress. Special *potential contact elements* are used to avoid the need to rearrange the FEM mesh due to variations of the contact surface as contact develops. Published results are used to validate the method, which is then applied to a turbine to solve the contact problem between the blade root and rotor in the region in which a 'push fit' connects the blade to its rotor.

Key words: elastic contact; contact surface element; potential contact element.

1. Introduction

The contact problem is one of the most challenging in solid mechanics. Since Kelvin's consideration of a point force acting on an infinite elastic space and Hertz's study of contact between two quadratically curved bodies, both of which took place a century ago, many researchers have concentrated on solving contact problems, ranging from classic complex function methods and integral equation methods to modern finite element and boundary element methods, i.e., FEM and BEM. FEM solutions have been developed by many researchers. Chen (1981) used a mixed FEM method to solve thermo-elastic contact problems, i.e., contact heat transfer and elastic contact conditions were considered simultaneously. Tan and Sha (1984) used a six noded triangular annular element and the wave front method to solve axisymmetric contact problems for spherical shells. Chen (1983) solved elasto-plastic contact problems, by using FEM, the mixed variational principle, quasi-elastic summation and double-iteration. Okamoto and Nakazawa (1979) considered the Coulomb type friction criterion and changed some elements in the stiffness matrix at each iteration in order to solve the contact problem for turbo-alternator end-bells. Fredriksson (1976) presented the incremental governing equations for linear elastic

† Visting Professor in the Division of Structural Engineering of the University of Wales Cardiff when this paper was written.
‡ Professor
‡† Researcher
‡‡ Lecturer

materials and solved them by using FEM and a super-element technique. Rahman (1984) applied loading iteration, contact condition iteration and friction condition iteration to solve special hole-edge contact problems. Torstenfelt (1984) discussed several issues related to the magnitude of loading steps. Cai and Liao (1993), Tseng and Olson (1981) and Haslinger and Hlavacek (1982) used a mixed FEM which treated both displacement and stress as degrees of freedom at nodes and they introduced contact force potential by means of Lagrangian multipliers. Oden and Pires (1983) developed a variational principle for nonlocal and nonlinear friction laws in elastic contact problems. Papadopoulos and Taylor (1993) and Kikuchi (1982) used a penalty method to satisfy the contact conditions and FEM to obtain the solution.

Zhong (1985a, 1985b) and Zhong and Sun (1989) deduced the minimum potential energy principle for elastic contact problems and solved the frictional contact problem by means of the parametric quadratic programming method. Im and Kawk (1993) used an auto-step-loading method in the linear programming method, considered interior and exterior slips caused by friction on a uniform contact surface and recommended the application of nonlinear programming to three-dimensional contact problems. Man *et al.* (1993), Paris *et al.* (1992) and Garrido *et al.* (1994) used an incremental BEM to solve frictional and/or non-frictional contact problems.

In this paper, the stiffness matrix of a two-dimensional contact surface element is first deduced, based on the principle of virtual work. Then, in order to reflect the variation of the contact surface, the incremental method is applied to control the loading procedure. The incremental loading factor (ILF) guarantees continuity of displacements and stress between each pair of contact nodes. *Potential contact elements* are introduced throughout the surface region where contact may occur, to avoid the need to rearrange the FEM mesh of nodes and elements as the contact surface varies during the loading procedure. Numerical examples are presented to validate the method by comparison with published results and finally the method is applied to solve the contact problem for turbines which occurs within the region in which a 'push fit' connects a blade to the rotor.

2. Two-dimensional contact surface element

2.1. Statement of the problem

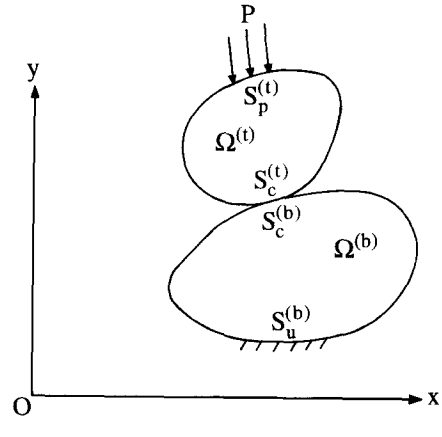

Fig. 1 Two bodies in contact

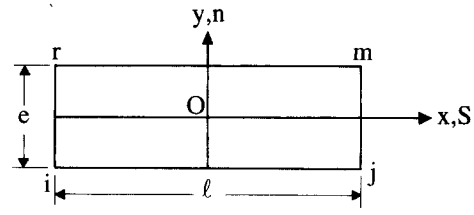

Fig. 2 Two-dimensional contact surface element

Consider two bodies $\Omega^{(\alpha)}$ (α=b, t) in contact, see Fig. 1. Note that for convenience, but without loss of generality, the contact surface has been taken as approximately horizontal, so that the superscripts b and t denote the bottom and top bodies, respectively. The bodies are bounded by the surfaces $S^{(\alpha)}$, which are divided into $S_u^{(\alpha)}$, $S_p^{(\alpha)}$ and $S_c^{(\alpha)}$ as follows. The displacements and the loads are assumed to be given on $S_u^{(\alpha)}$ and $S_p^{(\alpha)}$, respectively, while the bodies are in contact on $S_c^{(\alpha)}$. The bodies are assumed to be made of linearly elastic material, the displacements and strains are assumed to be small and the contact friction is assumed to obey Coulomb's law. Fig. 2 shows that in the local coordinate system S is the tangential line at the contact point and n is the outward normal vector from body $\Omega^{(b)}$ to body $\Omega^{(t)}$. The three alternative states of the contact are:

$$\sigma_n < 0, \ |\tau_s| < -\mu\sigma_n ,$$

i.e., the pair of contact nodes is sticking together;

$$\sigma_n < 0, \ |\tau_s| = -\mu\sigma_n ,$$

i.e., the pair of contact nodes are slipping over each other; and

$$\sigma_n > 0, \ \tau_s = 0,$$

i.e., the pair of contact nodes are separating from one another, i.e., the non-penetration condition is

$$g = v^A - v^B + \delta \geq 0$$

Here σ_n is the normal stress; τ_s is the tangential stress along S; μ is the friction coefficient on the contact surface between the two bodies; v^A and v^B are displacements along n of the pair of contact nodes A and B, with A on $\Omega^{(t)}$ and B on $\Omega^{(b)}$, respectively; and δ is the initial normal clearance between A and B.

2.2. Two-dimensional contact surface element

The contact problem is a locally nonlinear one because of the indeterminacy of the contact boundary and the key to solving it is the method used to represent accurately the crucial process of two elastic bodies that deform in conforming ways where they are in contact.

Fig. 2 shows a two-dimensional contact surface element comprising two contact surfaces ij and rm which both have length l and that are assumed to be linked by innumerable micro springs of height e, which becomes zero when the two bodies are in contact. The two top surface nodes r and m shown correspond to the bottom surface nodes i and j and the contact pair of nodes (A, B) is in turn (r, i) or (m, j). The top and bottom surfaces represent the contact

surfaces of the top and bottom bodies in Fig. 1 and the origin O of the local Cartesian coordinate system xy shown is at the centre of the element.

The node force and displacement vectors $\{F\}^e$ and $\{d\}^e$ are defined as, respectively,

$$\{F\}^e = [F_{xi}\ F_{yi}\ F_{xj}\ F_{yj}\ F_{xr}\ F_{yr}\ F_{xm}\ F_{ym}]^T$$
$$\{d\}^e = [u_i\ v_i\ u_j\ v_j\ u_r\ v_r\ u_m\ v_m]^T$$

where $\{F\}^e$ causes the small springs at distance x from O to have shear stress τ_s and normal stress σ_n, i.e.,

$$\{\sigma\} = [\tau_s\ \sigma_n]^T$$

The displacements of the bottom surface relative to the top surface cause the relative displacement $\{w\}$ to be

$$\{w\} = [u_b - u_t,\ v_b - v_t]^T$$

where the subscripts b and t denote the bottom and top surfaces, respectively. Because of the linear elastic assumption

$$\{\sigma\} = [D]\{w\} \tag{1}$$

where

$$[D] = \begin{bmatrix} E_s & 0 \\ 0 & E_n \end{bmatrix} \tag{2}$$

and E_s and E_n (which are independent of x) are, respectively, the tangential and normal stiffness coefficients of the contact surface element.

Assuming that the mode of displacement for each contact surface is a linear function of position x, then the displacements of the top and bottom surfaces are respectively defined as

$$[u_t\ v_t]^T = \frac{1}{2}[G]\,[u_r\ v_r\ u_m\ v_m]^T \tag{3}$$

$$[u_b\ v_b]^T = \frac{1}{2}[G]\,[u_i\ v_i\ u_j\ v_j]^T \tag{4}$$

where

$$\left.\begin{aligned} [G] &= \begin{bmatrix} \alpha & 0 & \beta & 0 \\ 0 & \alpha & 0 & \beta \end{bmatrix} \\ \alpha &= 1 - \frac{2x}{l}; \quad \beta = 1 + \frac{2x}{l} \end{aligned}\right\} \tag{5}$$

Therefore

$$\left.\begin{aligned} \{w\} &= [u_b - u_t\ v_b - v_t]^T = \frac{1}{2}[C]\{d\}^e \\ [C] &= [[G]\ \ -[G]] \end{aligned}\right\} \tag{6}$$

If a random virtual node displacement of $\{\delta d\}^e$ is assumed, then the relative virtual element displacement at x is

$$\{\delta w\} = \frac{1}{2}[C]\{\delta d\}^e$$

Because the virtual work of the element stresses is equal to that of the node forces,

$$\{\delta d\}^{eT}\{F\}^e = \int_{-l/2}^{l/2}\{\delta w\}^T\{\sigma\}dx = \frac{1}{4}\{\delta d\}^{eT}\int_{-l/2}^{l/2}[C]^T[D][C]\{d\}^e dx \tag{7}$$

where Eq. (1) has been used. Hence

$$\{F\}^e = [K]^e\{d\}^e \tag{8}$$

where

$$[K]^e = \frac{1}{4}\int_{-l/2}^{l/2}[C]^T[D][C]dx \tag{9}$$

From Eqs. (5), (6) and (9), the stiffness matrix $[K]^e$ is obtained as

$$[K]^e = \frac{l}{6}\begin{bmatrix} 2[D] & & \textit{Symm.} & \\ [D] & 2[D] & & \\ -2[D] & -[D] & 2[D] & \\ -[D] & -2[D] & [D] & 2[D] \end{bmatrix} \tag{10}$$

As with the stiffness matrix of an isoparametric element, the stiffness matrix of the contact surface element must undergo an axis transformation to allow for the contact surface of Fig. 1 not being horizontal before being assembled into the overall stiffness matrix of the entire structure according to the nodal equilibrium conditions. Hence the displacements of the entire structure can be obtained, enabling the stresses on the contact surface to be calculated.

2.3. Potential contact element

The contact state changes occasionally during the loading procedure, both because surface elements which were in contact may separate and also because previously separated surface elements may come into contact. This makes the problem complicated, e.g., it upsets FEM meshes due to new contact surface elements being produced while old ones disappear. In the present paper this problem is solved by introducing *potential contact elements* over that part of the gap between the two bodies over which contact may occur at some stage of the contact process, see Fig. 3. Their connection stiffnesses are zero if the two bodies are separated, i.e., $[D]$ becomes null. During loading, some potential contact elements become contact surface elements,

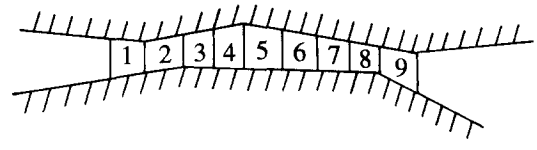

Fig. 3 Potential contact suface elements

i.e., the corresponding pairs of previously separated nodes make contact, whereas the reverse process occurs for other potential contact elements, corresponding to some pairs of nodes separating after being in contact.

3. Incremental loading procedure

3.1. Incremental loading factor (ILF)

At the typical i-th loading step the *Incremental Loading Factor* (ILF) β_i is chosen to be small enough to ensure that only a small variation of the contact surface occurs, such that if possible only one of the potential contact elements changes into a contact surface element or vice-versa. This is represented by $[D]$ changing from being null to having the value of Eq. (2) or vice-versa.

The incremental load for the i-th step is

$$\Delta F_i = \beta_i \Delta f_i \tag{11}$$

where Δf_i is a trial increment for which the structure is analysed using its contact state at the end of the (i-1)-th iteration. The choice of Δf_i does not alter the final results obtained.

After this incremental load, the load F_i, displacement v_i and normal stress σ_i in the system are, respectively,

$$F_i = F_{i-1} + \beta_i \Delta f_i \tag{12}$$

$$v_i = v_{i-1} + \beta_i \Delta v_i \tag{13}$$

$$\sigma_i = \sigma_{i-1} + \beta_i \Delta \sigma_i \tag{14}$$

where F_{i-1}, v_{i-1} and σ_{i-1} are the load, normal displacements and stress after the (i-1)-th step and Δv_i and $\Delta \sigma_i$ are the incremental displacement and stress due to the loading Δf_i.

From the non-penetrating condition defined in Section 2.1, if a potential element becomes a contact surface element at the i-th step then the *Incremental Displacement Factor* (IDF) is

$$\beta_{vi} = \frac{v_{i-1}^A - v_{i-1}^B + \delta}{\Delta v_i^A - \Delta v_i^B} \tag{15}$$

Here v_{i-1}^A and v_{i-1}^B are the normal displacements of the pair of nodes which make contact between the (i-1)-th and i-th steps and Δv_i^A and Δv_i^B are the normal incremental displacements of this pair of nodes due to Δf_i. If there is a chance of two or more pairs of nodes coming into contact between the (i-1)-th and i-th steps, Eq. (15) is repeated for each of them and the lowest value of β_{vi} so obtained is used.

The *Incremental Stress Factor* (ISF) β_{fi} at which a pair of nodes which was previously in contact separates is given by (Im and Kawk 1993)

$$\beta_{fi} = -\frac{\sigma_{n,i-1}}{\Delta \sigma_{n,i}} \tag{16}$$

where $\sigma_{n,i-1}$ is the normal stress of the pair of nodes after the (i-1)-th step and $\Delta \sigma_{n,i}$ is their normal incremental stress due to Δf_i. As for Eq. (15), if two or more pairs of nodes could separate between the (i-1)-th and i-th steps, Eq. (16) must be repeated for each of them and the

lowest value of β_{fi} so obtained is chosen.

The ILF β_i should satisfy both of the above IDF and ISF requirements simultaneously and so the ILF β_i for the i-th step is chosen to be

$$\beta_i = min.\ \{\beta_{vi}, \beta_{fi}\} \tag{17}$$

Note that the method presented assumes that the material is linear elastic throughout, but quite large deflections are permitted (and are used in the examples presented below) as the accumulation of the small deflection theory results for every loading step.

3.2. Values used for E_n and E_s

The stiffnesses E_s and E_n of Eq. (2) can be regarded as penalty factors, with their magnitudes reflecting the extent to which the contact conditions are satisfied. Therefore, E_n should be infinitely large whenever contact occurs. The high number used to represent this infinite value when computing must not be too large, because otherwise ill-conditioning occurs. Check results showed that acceptable results were obtained for any value in the approximate range $10^3 E_{max} < E_n < 10^8 E_{max}$, where E_{max} is the larger Young's modulus of either of the two bodies.

E_s should be obtained by iteration according to the slip condition

$$|\tau_s| = -\mu\sigma_n \tag{18}$$

so that, from Eqs. (1) and (2), the transition from sticking to sliding is represented by

$$E_{sj} = -\mu E_n \Delta v_j / |\Delta u_j|, \tag{19}$$

when computing the new values Δv_{j+1} and Δu_{j+1} from Eqs. (1) and (2), where j(=1, 2, ...) is the iteration number. These new values Δv_{j+1} and Δu_{j+1} are substituted in Eq. (19) and if the value of $E_{s,j+1}$ thus obtained is not sufficiently close to E_{sj} the calculations are repeated until adequate convergence is obtained.

4. Numerical examples for which published results are available

4.1. An elastic beam on an elastic foundation

To give a simple preliminary check against the published results of ГОРНОВ (1965), Fig. 4 shows his elastic beam with a uniformly distributed load and an elastic foundation. Because of the symmetry, only half of the structure was analysed. Fig. 5 shows the FEM mesh used for the structure, with the contact surface elements shown shaded. The beam and foundation are made of the same material, with Young's modulus E=200 GPa and Poisson's ratio ν=0.3. The contact surface is frictionless with $E_n \to \infty$, represented by $E_s = 10^{-5}E$ and $E_n = 10^5 E$. Fig. 4 shows the contact force R per unit length between the beam and its foundation compared to the results taken from ГОРНОВ (1965).

4.2. An elastic cylinder on an elastic foundation

Fig. 6 (a) shows an elastic cylinder on an elastic foundation that is square and rigidly supported. It was analysed as a frictionlesss interface plane strain problem and physically the

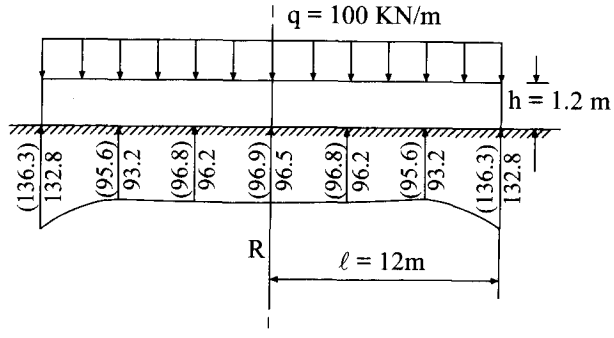

Fig. 4 Beam on elastic foundation, including results for R (in KN/m) obtained by the present method and (in brackets) by ГОРНОВ (1965)

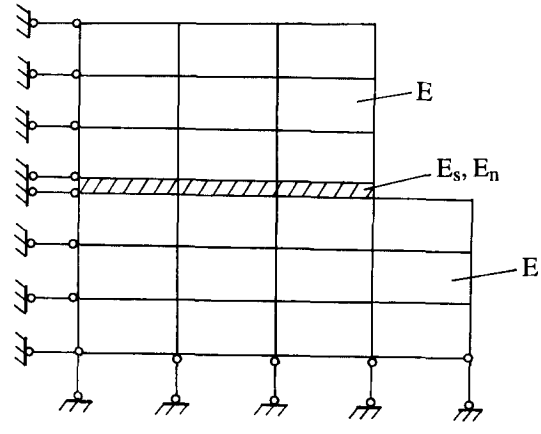

Fig. 5 FEM mesh for the right-hand half of the beam of Fig. 4 and its foundation, with the vertical scale exaggerated

initial state is a line contact which becomes an expanding rectangular contact as the external load is successively incremented. Only half of the structure is considered because of the symmetry and the line and rectangular contacts respectively become point and line contacts in the analysis. Fig. 6 (b) and (c) show the FEM meshes used. In Fig. 6(a), R=0.05 m, L=0.19 m and it is assumed that both solids have identical material properties of E=40 GPa and ν=0.35.

For P=41.76 KN/m, Table 1 gives results for the half contact width b and the maximum normal stress q_0 on the contact surface, compared with results from Hertz's analytical solution (Gladwell 1980) and with the results of Fredriksson (1976). Fig. 7 shows that the distribution of normal stress on the contact surface along the x-direction fits well with both Hertz's analytical solution and the results of Fredriksson (1976), while Fig. 8 gives the distribution in the y direction of the difference between the principal stresses σ_1 and σ_2.

4.3. An elastic punch on an elastic foundation

Fig. 9 shows an elastic punch on an elastic foundation, for which the dimensions are L_1=0.19 m and L_2=0.10 m. Because of the symmetry conditions, only half of the structure was analysed and the uniform punch compression load P_0=1.2 MPa. The solids have the identical elastic properties E=40 GPa and ν=0.35.

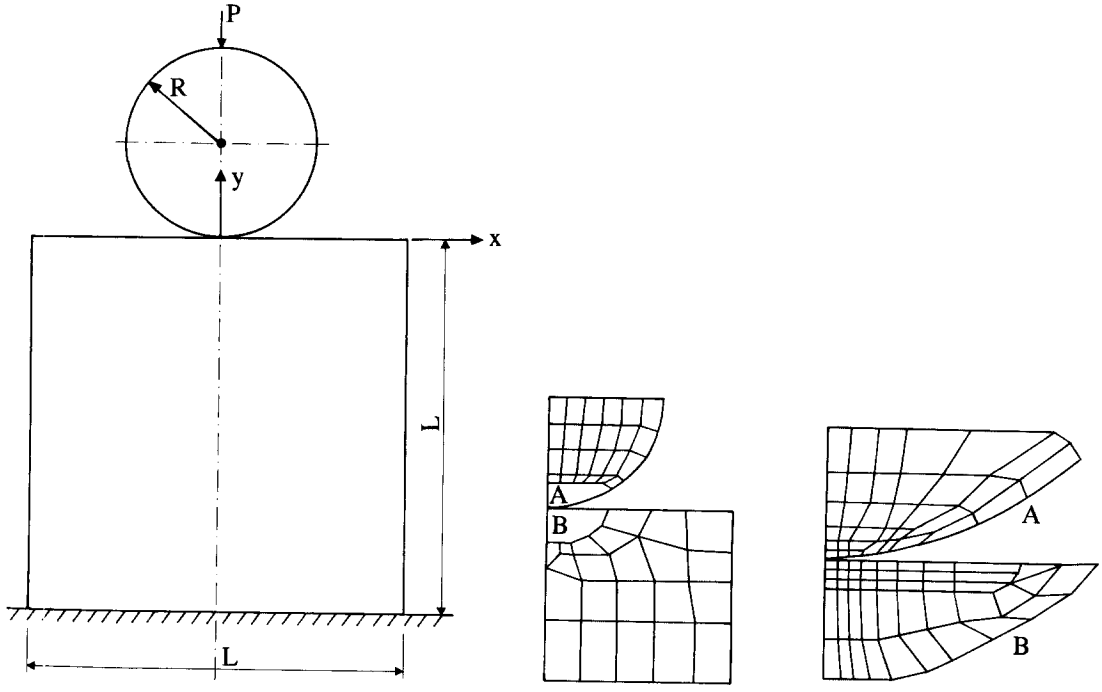

Fig. 6 An elastic cylinder on an elastic foundation showing (a) the problem; (b) an indication of the general mesh and; (c) an indication of the local mesh

Table 1 The maximum normal stress for the elastic cylinder on an elastic foundation

	Hertz	This paper	Fredriksson
b (10^{-3} m)	1.08	1.12	1.04
q_0 (MPa)	24.6	25.4	24.3

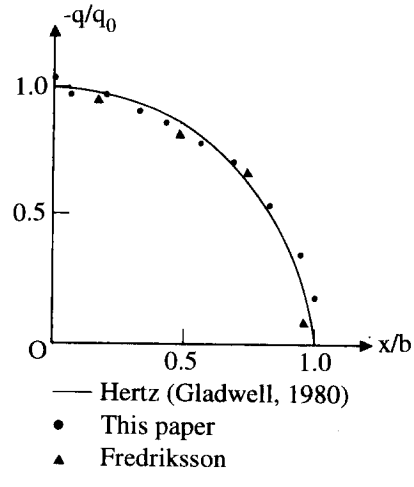

Fig. 7 Distribution of normal stress for the example of Fig. 6

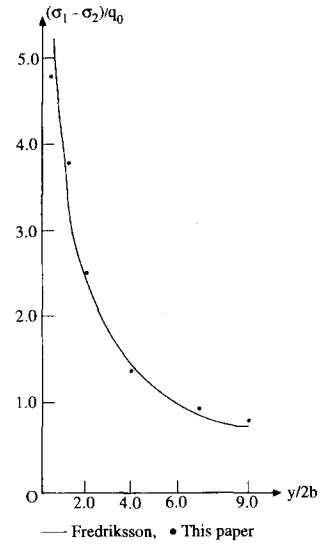

Fig. 8 Difference of principal stresses in ball at x=0

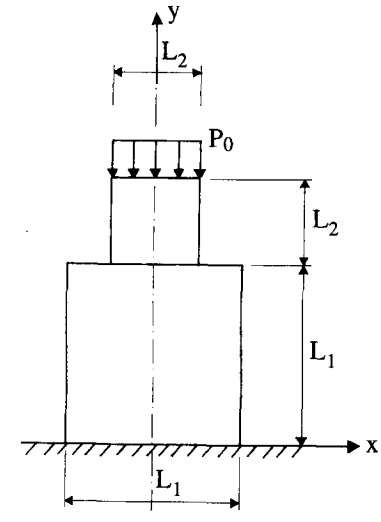

Fig. 9 A punch on a foundation

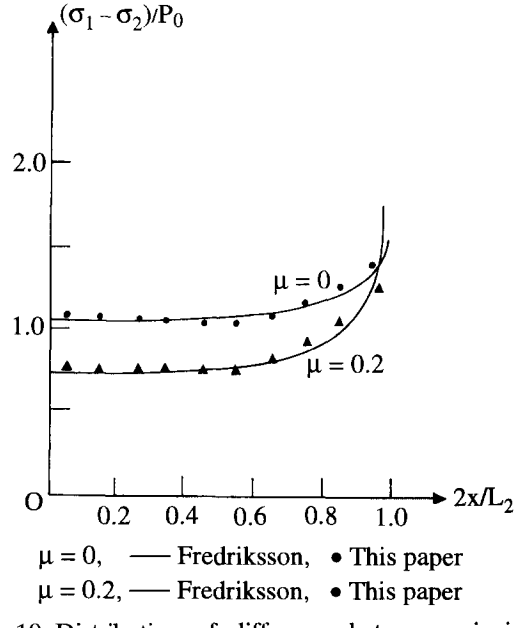

Fig. 10 Distribution of difference between principal stresses

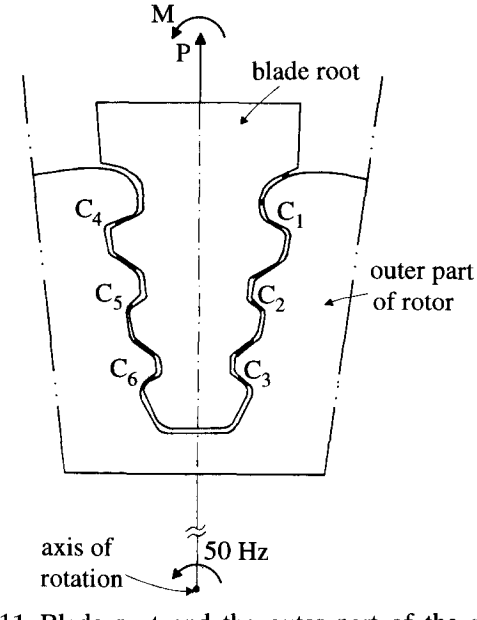

Fig. 11 Blade root and the outer part of the rotor that contains it

The results are presented and compared with those of Fredriksson (1976) in Fig. 10, where σ_1 and σ_2 are the principal stresses 1mm above the contact surface.

5. An application example

A high speed steam turbine has its blades connected to the outer part of the rotor by means of their roots, which are push fitted from the side, see Fig. 11. The forces acting on this connection

are the centrifugal force on the blade (which is by far the dominant one), the moment caused by the steam acting on the blade and the centrifugal forces on the blade root and the outer part of the rotor. These forces cause relatively high contact surface compressive stresses between the blade root and the outer part of the rotor.

Fig. 11 shows the portion of the outer part of the rotor considered along with the associated blade root.

The problem was treated as a plane strain one and Fig. 12 shows the mesh used for its cross-section. Due to the assumed distribution of the clearances, $C_1 \rightarrow C_6$ were the possible contact regions and they were represented by potential contact elements and contact surface elements. Elsewhere the clearance between the blade root and the outer part of the rotor was represented by potential contact elements which were constrained to always have $[D]=[0]$. The blade root and the outer part of the rotor were made of identical material, with Young's modulus E=200 GPa, Poisson's ratio ν=0.3, density $\rho=7.83\times10^3$ kg/m^3 and a friction coefficient between them μ=0.2. The total load included a centrifugal force on the blade of P=6280.15 N, moment M= 1.5868 N-m and the distributed centrifugal forces on the blade root and the outer part of the rotor, which was rotating at 50 Hz. The trial load increment Δf_i was 10% of the total load q_0 and the initial contact state was assumed to be $C_1=C_4=0$ and C_2, C_3, C_5, $C_6>0$, where $C_i=0$ and $C_i>0$ respectively indicate that the region C_i is always represented as a contact surface element or is represented by a potential contact element.

Table 2 shows the loading process and results, which should be self explanatory, except that σ_{max} is the principal stress at the most heavily stressed position in the blade root or rotor at each step, e.g., after the first four loading steps the load is 28% of the total load (i.e., 28% q_0) and $C_1 \rightarrow C_6=0$. Then, as the fifth and final load step, the load increases further to 100% of the total load (i.e., to 100% q_0) with no contact surface elements separating.

Fig. 13 shows the distribution of the maximum principal stress after all loading steps. The

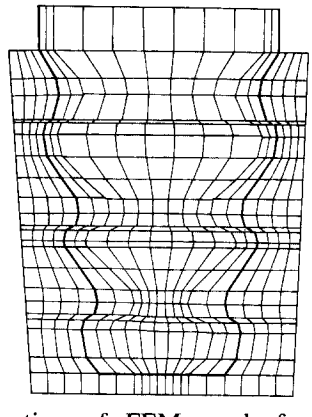

Fig. 12 Indication of FEM mesh for the cross-section

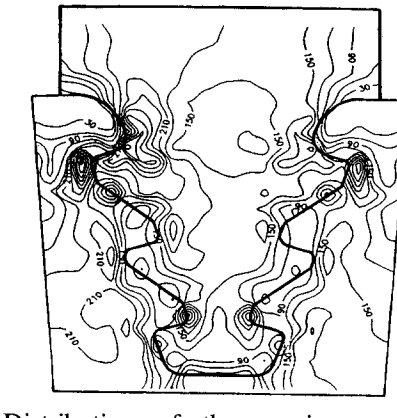

Fig. 13 Distribution of the maximum principal stress, in MPa

Table 2 The loading process for the turbine problem

New contact at	C_6	C_3	C_5	C_2	None
ILF β_i	1.58	0.28	0.41	0.53	7.20
$\Delta\sigma_{max}$ (MPa)	400.37	41.96	42.72	42.82	526.62
σ_{max} (MPa)	400.37	442.33	485.05	527.87	1054.49

structure and the centrifugal force are symmetric and the distribution of the maximum principal stress is nearly symmetric. The small lack of symmetry is due to the moment, which is very small compared to the centrifugal force, e.g., the maximum node load that it causes is only 4% of that caused by the centrifugal force.

6. Conclusions

The variation of the contact surface can be reflected very accurately by using the contact surface elements, the potential contact elements and the incremental method presented in this paper. The method avoids the need to rearrange the FEM mesh, i.e., nodes and elements, during the loading procedure. The results presented show that the method is quite accurate.

Acknowledgements

This work was supported in part by the Foundation for Promoting Cultural, Education and Technical Co-operation between Britain and China and by the Cardiff Advanced Chinese Engineering Centre.

References

Cai, Z.X. and Liao, C.L. (1993), "Two-dimensional contact stress analysis using mixed finite element method", *J. of Taiwan Mechanics Association,* **9**(4), 319-330. (in Chinese)

Chen, M.Q. (1983), "Solution of elasto-plastic contact problems using quasi-elastic summation and double-iteration", *J. of Solid Mechanics,* **3**, 365-374. (in Chinese)

Chen, W.J. (1981), "An analysis of coupled thermal-elastic contact problems with the finite element method", *J. of Solid Mechanics,* **3**, 326-336. (in Chinese)

Fredriksson, B. (1976), "Finite element solution of surface nonlinearities in structural mechanics with special emphasis to contact and fracture mechanics problems", *Computers & Structures,* **6**, 281-290.

Garrido, J.A., Foces, A. and Paris, F. (1994), "An incremental procedure for three-dimensional contact problems with friction", *Computers & Structures,* **50**(2), 201-215.

Gladwell, G.M.L. (1980), *Contact Problems in the Classical Theory of Elasticity,* Sijthoff and Noordogg.

Haslinger, J. and Hlavacek, I. (1982), "Approximation of the Signorini problem with friction by a mixed finite element method", *J. Math. Analys. Appl.,* **86**, 99-122.

Im, S.B. and Kawk, B.M. (1993), "Sensitivity analysis for automatic loading in frictional contact formulated by complementarity", *Computers & Structures,* **46**(2), 355-364.

Kikuchi, N. (1982), "A smoothing technique for reduced integration penalty methods in contact problem", *Int. J. Num. Eng.,* **18**, 343-350.

Man, K.W., Aliabadi, M.H. and Rooke, D.P. (1993), "BEM frictional contact analysis: load incremental technique", *Computers & Structures,* **47**(6), 893-905.

Oden, J.T. and Pires, E.B. (1983), "Nonlocal and nonlinear friction laws and variational principles for contact problems in elasticity", *J. Appl. Mechs. Trans. ASME,* **50**, 67-76.

Okamoto, N. and Nakazawa, M. (1979), "Finite element incremental contact analysis with various frictional conditions", *Int. J. Num. Meth. Eng.* **14**, 337-357.

Papadopoulos, P. and Taylor, R.L. (1993), "A simple algorithm for three-dimensional finite element analysis of contact problems", *Computers & Structures,* **46**(6), 1107-1118.

Paris, F., Foces A. and Garrido, J.A. (1992), "Application of boundary element method to solve three-dimensional elastic contact problems without friction", *Computers & Structures,* **43**(1), 19-30.

Rahman, M.U. (1984), "An iterative procedure for finite element stress analysis of frictional contact problems", *Computers & Structures,* **18**(6), 947-954.

Tan, L.S. and Sha, X.H. (1984), "Finite element analysis of elastic contact problem of axisymmetric opening in spherical shell", *J. of Solid Mechanics,* **2**, 262-268. (in Chinese)

Torstenfelt, B.R. (1984), "An automatic incrementation technique for contact problems with friction", *Computers & Structures,* **19**(3), 393-400.

Tseng, J. and Olson, M.D. (1981), "The mixed finite element method applied to two-dimensional elastic contact problems", *Int. J. Num. Meth. Eng.,* **17**, 991-1014.

Zhong, W.X. (1985a), "The minimum potential energy principle in elastic contact problems and its numerical method", *Comput. Struct. Mech. and Appl.,* **2**(1), 21-29. (in Chinese)

Zhong, W.X. (1985b), "On variation principle of elastic contact problems and parametric quadratic programming solution", *Comput. Struct. Mech. and Appl.,* **2**(2), 1-10. (in Chinese)

Zhong, W.X. and Sun, S.M. (1989). "A parametric quadratic programming approach to elastic contact problems with friction", *Computers & Structures,* **32**(1), 37-43.

ГОРНОВ, M. (1965), *Calculation of Structures on Elastic Foundation,* China Industry Press.